JOURNAL OF SPACECRAFT AND ROCKETS
Vol. 43, No. 4, July–August 2006

Engineering Notes

ENGINEERING NOTES are short manuscripts describing new developments or important results of a preliminary nature. These Notes should not exceed 2500 words (where a figure or table counts as 200 words). Following informal review by the Editors, they may be published within a few months of the date of receipt. Style requirements are the same as for regular contributions (see inside back cover).

Classical Orbit Element Differences Determination Using Relative Position Coordinates

Zhe Dong* and Zheng You†
Tsinghua University, 100084 Beijing, People's Republic of China
and
Xiaomin Zhang‡
DFH Satellite Corporation, 100086 Beijing, People's Republic of China

Introduction

SPACECRAFT formation flying is a powerful technology envisioned for many future space science missions such as virtual platforms for Earth observations and clusters for magnetospheric exploration and enhanced stellar optical interferometers.[1,2] To describe a relative motion between the deputy and the chief, two coordinate sets are traditionally utilized. A common choice is to use the local-vertical–local-horizontal (LVLH) coordinate frame, and the six Cartesian initial conditions are the invariant parameters of a relative orbit. An alternate set of six invariant parameters utilized to describe the relative orbit is the classical orbit element differences between the deputy and the chief. Because unperturbed classical orbit element differences between the deputy and the chief, that is, the differences between the semimajor axis, eccentricity, inclination, right ascension of the ascending node, argument of perigee, and initial mean anomaly of the deputy and that of the chief, are constant and can be compared to their nominal values at any time, it is more convenient to describe the relative orbit in terms of classical orbit element differences than to do that in terms of local Cartesian initial conditions. Schaub presented a general estimation method for the linearized relative orbit geometry of spacecraft formations about a circular or an elliptic reference orbit,[3] and the relative orbit is described purely through orbit element differences between the chief and the deputy. Several relative orbit control laws of which the feedback variables are orbit element differences have been explored in the last several years.[4–6] Thus, the problem of how to determine orbit element differences using relative motion states and orbit elements of the chief is a key problem to be solved. Several researchers have investigated the problem in the last several years. Alfriend et al. proposed a linearized mapping that maps the Cartesian position and velocity coordinates in the LVLH coordinate frame to the classical orbit element differences.[7] Gim and Alfriend expanded this work and presented a state transition matrix for relative motion when the reference orbit is elliptic and both satellites are subjected to the J_2 perturbation.[8] By the use of various celestial mechanics properties, Schaub and Alfriend presented a direct approach that maps the orbit element differences to the local Cartesian position and velocity coordinates and designed a hybrid feedback control law in terms of both the local Cartesian position and velocity coordinates and the desired orbit element differences.[9]

This paper presents a novel approach that maps local Cartesian position coordinates of N ($N \geq 4$) points on a relative orbit to classical orbit element differences between the deputy and the chief. The only assumption made here is that N ($N \geq 4$) measurements of the deputy's relative position and the chief's orbit elements are given. The main difference between this approach and the aforementioned methods is that this approach does not need local Cartesian velocity information, that is, this approach can be utilized to determinate the classical orbit element differences between the deputy and the chief with only relative position information.

Relationship Between Relative Orbit and Orbit Elements of Deputy Spacecraft

To study the relative motion between the deputy and the chief, two coordinate frames are shown in Fig. 1. Here, $O_eX_eY_eZ_e$ is the Earth-centered inertial (ECI) coordinate frame. $Oxyz$ is the LVLH coordinate frame with the origin O at the mass center of the chief satellite (the chief in Fig. 1). Axis Ox points radially outward from the Earth's center. Axis Oy is in the in-track direction along increasing true anomaly. This right-handed coordinate frame is completed with axis Oz pointing in the cross-track direction.

The reference orbit in the ECI coordinate frame is represented by a, e_1, i_1, Ω_1, ω_1, and M_{10}, which correspond to the semimajor axis, eccentricity, inclination, right ascension of the ascending node, argument of perigee, and initial mean anomaly of the reference orbit. The transform matrix from $O_eX_eY_eZ_e$ to $Oxyz$ can be represented

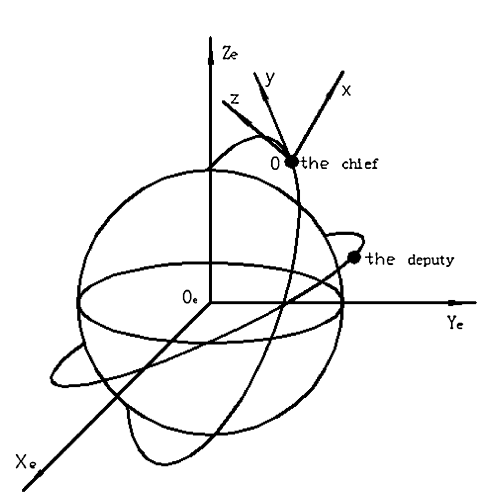

Fig. 1 ECI and LVLH coordinate systems.

Received 14 April 2005; revision received 4 August 2005; accepted for publication 8 September 2005. Copyright © 2006 by the American Institute of Aeronautics and Astronautics, Inc. All rights reserved. Copies of this paper may be made for personal or internal use, on condition that the copier pay the $10.00 per-copy fee to the Copyright Clearance Center, Inc., 222 Rosewood Drive, Danvers, MA 01923; include the code 0022-4650/06 $10.00 in correspondence with the CCC.

*Ph.D. Student, Department of Precision Instrument and Mechanology; dz98@mails.tisnghua.edu.cn.
†Professor, Department of Precision Instrument and Mechanology; yz-dpi@mail.tsinghua.edu.cn. Member AIAA.
‡Associate Professor; Zhangxiaomin01@tsinghua.org.cn.

as

$$U_1 = R_3(u_1)R_1(i_1)R_3(\Omega_1) \tag{1}$$

where

$$u_1 = \omega_1 + f_1, \qquad R_3(\cdot) = \begin{bmatrix} \cos(\cdot) & \sin(\cdot) & 0 \\ -\sin(\cdot) & \cos(\cdot) & 0 \\ 0 & 0 & 1 \end{bmatrix}$$

$$R_1(\cdot) = \begin{bmatrix} 1 & 0 & 0 \\ 0 & \cos(\cdot) & \sin(\cdot) \\ 0 & -\sin(\cdot) & \cos(\cdot) \end{bmatrix}$$

and f_1 is the true anomaly of the chief.

Substitute $R_3(u_1)$, $R_1(i_1)$, and $R_3(\Omega_1)$ into Eq. (1):

$$U_1 = \begin{bmatrix} \cos\Omega_1\cos u_1 - \cos i_1 \sin\Omega_1 \sin u_1 & \sin\Omega_1 \cos u_1 + \cos i_1 \cos\Omega_1 \sin u_1 & \sin i_1 \sin u_1 \\ -\cos\Omega_1 \sin u_1 - \cos i_1 \sin\Omega_1 \cos u_1 & -\sin\Omega_1 \sin u_1 + \cos i_1 \cos\Omega_1 \cos u_1 & \sin i_1 \cos u_1 \\ \sin i_1 \sin\Omega_1 & -\sin i_1 \cos\Omega_1 & \cos i_1 \end{bmatrix} \tag{2}$$

The companion orbit in the ECI coordinate frame is represented by a, e_2, i_2, Ω_2, ω_2, and M_{20}, which correspond to the semimajor axis, eccentricity, inclination, right ascension of the ascending node, argument of perigee, and initial mean anomaly of the companion orbit. Let $[x_{e1} \ \ y_{e1} \ \ z_{e1}]^T$ and $[x_{e2} \ \ y_{e2} \ \ z_{e2}]^T$ be the position coordinates of the chief and the deputy in the ECI coordinate frame, respectively, and let $[x \ \ y \ \ z]^T$ be the position coordinates of the deputy in the LVLH coordinate frame $Oxyz$. Then the equation of relative kinematics is

$$\begin{bmatrix} x \\ y \\ z \end{bmatrix} = U_1 \begin{bmatrix} x_{e2} \\ y_{e2} \\ z_{e2} \end{bmatrix} - \begin{bmatrix} r_{e1} \\ 0 \\ 0 \end{bmatrix} \tag{3}$$

where

$$\begin{bmatrix} x_{e2} \\ y_{e2} \\ z_{e2} \end{bmatrix} = r_{e2} \begin{bmatrix} \cos(\omega_2 + f_2)\cos\Omega_2 - \cos i_2 \sin(\omega_2 + f_2)\sin\Omega_2 \\ \cos(\omega_2 + f_2)\sin\Omega_2 - \cos i_2 \sin(\omega_2 + f_2)\cos\Omega_2 \\ \sin i_2 \sin(\omega_2 + f_2) \end{bmatrix}$$

$$r_{ei} = \sqrt{x_{ei}^2 + y_{ei}^2 + z_{ei}^2}, \qquad i = 1 \quad \text{or} \quad 2$$

The orbital coordinate frame $O_e x' y' z'$ is shown in Fig. 2. Axis $O_e x'$ points radially toward the perigee of the deputy. Axis $O_e z'$ is aligned with the angular momentum vector of the chief. This right-handed coordinate frame is completed with axis $O_e y$. Let $[x' \ \ y' \ \ z']^T$ be the position coordinates of the deputy in $O_e x' y' z'$. The transform matrix from $O_e X_e Y_e Z_e$ to $O_e x' y' z'$ is $U_2 = R_3(\omega_2)R_1(i_2)R_3(\Omega_2)$, namely,

$$U_2 = \begin{bmatrix} \cos\Omega_2\cos\omega_2 - \cos i_2 \sin\Omega_2 \sin\omega_2 & \sin\Omega_2 \cos\omega_2 + \cos i_2 \cos\Omega_2 \sin\omega_2 & \sin i_2 \sin\omega_2 \\ -\cos\Omega_2 \sin\omega_2 - \cos i_2 \sin\Omega_2 \cos\omega_2 & -\sin\Omega_2 \sin u_2 + \cos i_2 \cos\Omega_2 \cos\omega_2 & \sin i_2 \cos\omega_2 \\ \sin i_2 \sin\Omega_2 & -\sin i_2 \cos\Omega_2 & \cos i_2 \end{bmatrix} \tag{4}$$

From Eq. (4), we have

$$\begin{bmatrix} x' \\ y' \\ z' \end{bmatrix} = U_2 \begin{bmatrix} x_{e2} \\ y_{e2} \\ z_{e2} \end{bmatrix} \tag{5}$$

$$\left[(x' - ae_2)^2 \big/ a^2\right] + \left[y'^2 \big/ a^2\left(1 - e_2^2\right)\right] = 1 \tag{6}$$

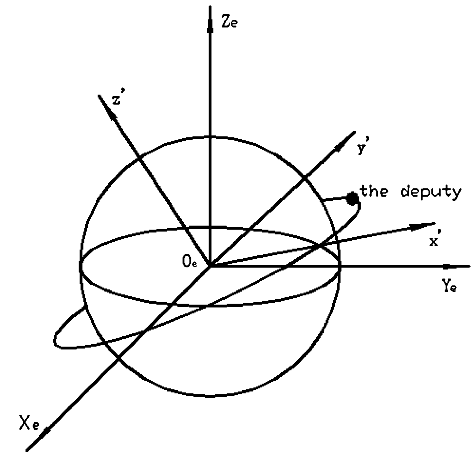

Fig. 2 Orbital coordinate system $O_e x' y' z'$.

$$z' = 0 \tag{7}$$

Consider Eqs. (5) and (7); we can obtain

$$z_{e2} = [y_{e2} \quad -x_{e2}] \begin{bmatrix} \tan i_2 \cos\Omega_2 \\ \tan i_2 \sin\Omega_2 \end{bmatrix} \tag{8}$$

$$\begin{bmatrix} x' \\ y' \end{bmatrix} = \begin{bmatrix} \alpha & \beta \\ \beta & -\alpha \end{bmatrix} \begin{bmatrix} \cos\omega_2 \\ \sin\omega_2 \end{bmatrix} \tag{9}$$

where

$$\alpha = x_{e2}\cos\Omega_2 + y_{e2}\sin\Omega_2$$

$$\beta = -x_{e2}\cos i_2 \sin\Omega_2 + y_{e2}\cos i_2 \cos\Omega_2 + z_{e2}\sin i_2 \tag{10}$$

From Eq. (6)

$$(x'^2 + y'^2)\big/a^2 - 1 = [(x'^2/a^2 - 2)(2x'/a)1]\boldsymbol{e} \tag{11}$$

where $\boldsymbol{e} = [e_2^2(e_2 - e_2^3)e_2^4]^T$.

Because $z_{e2} = r_{e2}\sin(\omega_2 + f_2)\sin(i_2)$, we can obtain the eccentric anomaly of the deputy E_2, that is,

$$E_2 = 2\arctan\left\{\sqrt{(1 - e_2)/(1 + e_2)} \times \tan\left[\tfrac{1}{2}\arcsin(z_{e2}/r_{e2}\sin i_2) - \tfrac{1}{2}\omega_2\right]\right\} \tag{12}$$

Let $[x_{e20} \ y_{e20} \ z_{e20}]^T$ be the initial position coordinates of the chief in the ECI coordinate frame, and let E_{10} and E_{20} be the eccentric anomalies of the chief and the deputy, respectively. It is assumed that E_{10} is given. Then from Eq. (12), we can obtain

$$E_{20} = 2\arctan\left\{\sqrt{(1 - e_2)/(1 + e_2)} \times \tan\left[\tfrac{1}{2}\arcsin\left(z_{e20}/r_{e20}\sin i_2\right) - \tfrac{1}{2}\omega_2\right]\right\} \tag{13}$$

Moreover, the mean anomaly of the deputy is

$$M_{20} = E_{20} - e_2 \sin(E_{20}) \tag{14}$$

In the next section, we present an approach that obtains the estimation or calculated values of Ω_2, i_2, e_2, and M_{20} from Eqs. (8), (10), (11), and (13) with the value of ω_2, relative position coordinates of N ($N \geq 4$) different points on a relative orbit, and orbit elements of the chief.

Least-Squares Estimation of Ω_2, i_2, e_2, and M_{20}

It is assumed that the argument of perigee of the deputy orbit ω_2, orbit elements of the chief, and relative position coordinates of N ($N \geq 4$) different points on the relative orbit are given. Because an arbitrary set of points in the LVLH coordinate frame may be not on a same Keplerian elliptical orbit, we employ the least-squares estimation method to estimate Ω_2, i_2, and e_2, and then calculate the deputy's initial mean anomaly.

Let $\boldsymbol{x}_{0k} = [x_{0k} \;\; y_{0k} \;\; z_{0k}]^T$, $k = 1, 2, \ldots, N$, be the measurement values of the relative position coordinates of N ($N \geq 4$) different points on the relative orbit, and let the corresponding radius relative to the Earth of the reference orbit be r_{e1k}, $k = 1, 2, \ldots, N$. Then the corresponding position coordinates of the N ($N \geq 4$) different points in the ECI coordinate frame can be represented as

$$\begin{bmatrix} x_{e2k} \\ y_{e2k} \\ z_{e2k} \end{bmatrix} = \boldsymbol{U}_{1k}^T \left(\begin{bmatrix} x_{0k} \\ y_{0k} \\ z_{0k} \end{bmatrix} + \begin{bmatrix} r_{e1k} \\ 0 \\ 0 \end{bmatrix} \right), \quad k = 1, 2, \ldots, N \tag{15}$$

where

$$\boldsymbol{U}_{1k} = \begin{bmatrix} \cos\Omega_1 \cos(\omega_1 + f_{1k}) - \cos i_1 \sin\Omega_1 \sin(\omega_1 + f_{1k}) & \sin\Omega_1 \cos(\omega_1 + f_{1k}) + \cos i_1 \cos\Omega_1 \sin(\omega_1 + f_{1k}) & \sin i_1 \sin(\omega_1 + f_{1k}) \\ -\cos\Omega_1 \sin(\omega_1 + f_{1k}) - \cos i_1 \sin\Omega_1 \cos(\omega_1 + f_{1k}) & -\sin\Omega_1 \sin(\omega_1 + f_{1k}) + \cos i_1 \cos\Omega_1 \cos(\omega_1 + f_{1k}) & \sin i_1 \cos(\omega_1 + f_{1k}) \\ \sin i_1 \sin\Omega_1 & -\sin i_1 \cos\Omega_1 & \cos i_1 \end{bmatrix}$$

and f_{1k} is the chief's true anomaly corresponding to r_{e1k}.

Let t_{1k} be the time corresponding to r_{e1k}, which satisfies

$$t_{1k} = \sqrt{a^3/\mu}(E_{1k} - e_1 \sin E_{1k} - M_{10}), \qquad t_{11} = 0 \tag{16}$$

where μ is the gravitational constant of the Earth and E_{1k} is the eccentric anomaly corresponding to r_{e1k}, which satisfies

$$E_{1k} = 2 \arctan\left[\sqrt{(1 - e_1)/(1 + e_1)} \tan(f_{1k}/2)\right] \tag{17}$$

From Eq. (9), the estimation values of the right ascension of the ascending node Ω_2 and the inclination i_2 of the deputy are

$$\hat{\Omega}_2 = \arctan(t_2/t_1)$$
$$\hat{i}_2 = \arctan(t_1/\cos\hat{\Omega}_2) \tag{18}$$

where

$$\boldsymbol{t} = \begin{bmatrix} t_1 \\ t_2 \end{bmatrix} = (\boldsymbol{A}^T \boldsymbol{A})^{-1} \boldsymbol{A}^T \boldsymbol{b}$$

$$\boldsymbol{A} = \begin{bmatrix} y_{e21} & -x_{e21} \\ y_{e22} & -x_{e22} \\ \vdots & \vdots \\ y_{e2N} & -x_{e2N} \end{bmatrix}, \qquad \boldsymbol{b} = \begin{bmatrix} z_{e21} \\ z_{e22} \\ \vdots \\ z_{e2N} \end{bmatrix}$$

Here, $\hat{\Omega}_2$, $\hat{i}_2$, t_1, and t_2 are the estimation values of Ω_2, i_2, $(\tan i_2 \cos\Omega_2)$, and $(\tan i_2 \sin\Omega_2)$, respectively.

From Eqs. (9) and (11), the estimation value of the eccentricity of the deputy orbit is

$$\hat{e}_2 = \sqrt{\hat{\boldsymbol{e}}(1)} \tag{19}$$

where

$$\hat{\boldsymbol{e}} = (\boldsymbol{Y}^T \boldsymbol{Y})^{-1} \boldsymbol{Y}^T \boldsymbol{z} = [\hat{\boldsymbol{e}}(1) \quad \hat{\boldsymbol{e}}(2) \quad \hat{\boldsymbol{e}}(3)]^T \tag{20}$$

$$\boldsymbol{Y} = \begin{bmatrix} \dfrac{x_1'^2}{a^2} - 2 & \dfrac{2x_1'}{a} & 1 \\ \dfrac{x_2'^2}{a^2} - 2 & \dfrac{2x_2'}{a} & 1 \\ \vdots & \vdots & \vdots \\ \dfrac{x_N'^2}{a^2} - 2 & \dfrac{2x_N'}{a} & 1 \end{bmatrix}_{N \times 3} \tag{21}$$

$$\boldsymbol{z} = \begin{bmatrix} \dfrac{x_1'^2 + y_1'^2}{a^2} - 1 & \dfrac{x_2'^2 + y_2'^2}{a^2} - 1 & \cdots & \dfrac{x_N'^2 + y_N'^2}{a^2} - 1 \end{bmatrix}_{1 \times N} \tag{22}$$

$$\begin{bmatrix} x_k' \\ y_k' \end{bmatrix} = \begin{bmatrix} \alpha_k & \beta_k \\ \beta_k & -\alpha_k \end{bmatrix} \begin{bmatrix} \cos\omega_2 \\ \sin\omega_2 \end{bmatrix} \tag{23}$$

$$\alpha_k = x_{e2k} \cos\hat{\Omega}_2 + y_{e2k} \sin\hat{\Omega}_2$$
$$\beta_k = -x_{e2k} \cos\hat{i}_2 \sin\hat{\Omega}_2 + y_{e2k} \cos\hat{i}_2 \cos\hat{\Omega}_2 + z_{e2k} \sin\hat{i}_2$$
$$(k = 1, 2, \cdots, N) \tag{24}$$

Furthermore, the estimation value of M_{20} is

$$\hat{M}_{20} = \hat{E}_{20} - \hat{e}_2 \sin(\hat{E}_{20}) \tag{25}$$

where

$$\hat{E}_{20} = 2 \arctan\left\{\sqrt{(1 - \hat{e}_2)/(1 + \hat{e}_2)} \times \tan\left[\tfrac{1}{2} \arcsin(z_{e20}/r_{e20} \sin\hat{i}_2) - \tfrac{1}{2}\hat{\omega}_2\right]\right\} \tag{26}$$

Searching Algorithm for Argument of Perigee of Deputy

From Eqs. (18), (19), and (25), the estimation or calculated values of Ω_2, i_2, e_2, and M_{20} are obtained on the assumption that ω_2 is known, and from Eq. (23) we can see that the error of ω_2 causes the errors of the estimation value $\hat{e}_2$ and the calculated value $\hat{M}_{20}$. Furthermore, we can calculated the relative position coordinates using a, $\hat{e}_2$, $\hat{i}_2$, $\hat{\Omega}_2$, $\hat{M}_{20}$, and the guess value of ω_2, and then we can conclude that the difference between the guess and actual values of ω_2 causes the difference between the calculated and measurement relative position coordinates. Thus, to minimize the difference between the calculated and measurement relative position coordinates, we can search the value of ω_2 in a neighborhood of ω_1.

Let $\boldsymbol{q}_{0k} = [u_{0k} \;\; v_{0k} \;\; w_{0k}]^T$, $k = 1, 2, \ldots, N$, be calculated values of the relative position coordinates corresponding to a searching value of ω_2. From Eq. (18), $\hat{\Omega}_2$ and $\hat{i}_2$ can be obtained using the measurement relative position values $\boldsymbol{x}_{0k}$, $k = 1, 2, \ldots, N$. Let ω_{2f} be a searching value of ω_2, and then from Eqs. (19) and (25), we can obtain $\hat{e}_{2f}$ and $\hat{M}_{20f}$, which are the estimation values of the eccentricity and the initial mean anomaly, respectively. Furthermore, $\boldsymbol{q}_{0k}$ can be obtained using the following equations:

$$\begin{bmatrix} u_{0k} \\ v_{0k} \\ w_{0k} \end{bmatrix} = \frac{a\left(1-\hat{e}_{2f}^2\right)}{1+\hat{e}_{2f}\cos f_{2k}}$$

$$\boldsymbol{U}_{1k}\begin{bmatrix} \cos(\omega_{2f}+f_{2k})\cos\hat{\Omega}_2 - \cos i_2 \sin(\omega_{2f}+f_{2k})\sin\hat{\Omega}_2 \\ \cos(\omega_{2f}+f_{2k})\sin\hat{\Omega}_2 - \cos i_2 \sin\left(\omega_{2f}+f_{2k_2}\right)\cos\hat{\Omega}_2 \\ \sin\hat{i}_2 \sin(\omega_{2f}+f_{2k}) \end{bmatrix}$$

$$-\begin{bmatrix} r_{e1k} \\ 0 \\ 0 \end{bmatrix} \tag{27}$$

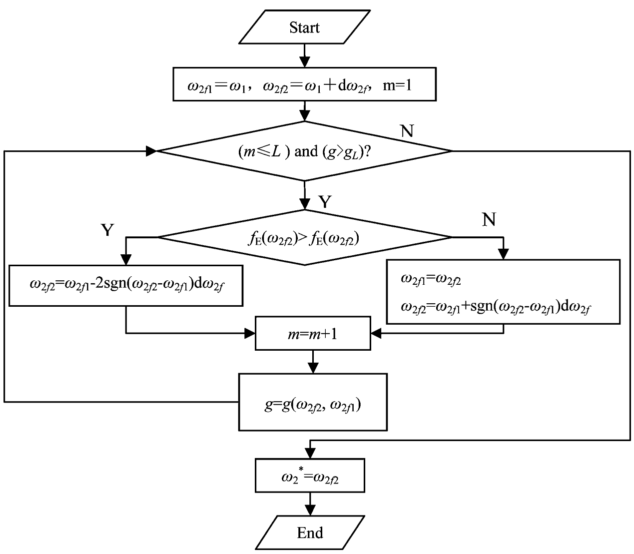

Fig. 3 Flow process chart of searching algorithm of ω_2.

$$f_{2k} = 2\arctan\left[\sqrt{(1+\hat{e}_{2f})/(1-\hat{e}_{2f})}\tan(E_{2k}/2)\right] \tag{28}$$

$$E_{2k} - \hat{e}_{2f}\sin E_{2k} = M_{2k} \tag{29}$$

$$M_{2k} = \sqrt{\mu/a^3}(t_{2k} + \hat{M}_{20f}) \tag{30}$$

where f_{2k}, E_{2k}, and M_{2k} are the deputy's calculated true, eccentric, and mean anomalies and t_{2k} is the corresponding time that satisfies $t_{1k} = t_{2k}$. Define the evaluation function of ω_{2f} as

$$f_E(\omega_{2f}) = \sum_{k=1}^{N}\left\|\boldsymbol{x}_{0k} - \boldsymbol{q}_{0k}\right\|_2^2 = \sum_{k=1}^{N}\left[(x_{0k}-u_{0k})^2 + (y_{0k}-v_{0k})^2 + (z_{0k}-w_{0k})^2\right] \tag{31}$$

From Eq. (31), $f_E(\omega_{2f})$ describes the magnitude of the difference between the calculated and measurement relative position coordinates. We can see that $f_E(\omega_{2f})$ is smaller, and the guess value of the deputy's argument of perigee ω_{2f} is closer to its actual value.

Let ω_{2f1} and ω_{2f2} be two different searching values of ω_2 in the searching process, and let ω_2^* be the searching result of ω_2. Moreover, let L and $\mathrm{d}\omega_{2f}$ be the maximal iterative times and step length of the algorithm, respectively, and let m denote the iterative times. Define the iterative process function g as

$$g(\omega_{2f2}, \omega_{2f1}) = \frac{|f_E(\omega_{2f2}) - f_E(\omega_{2f1})|}{f_E(\omega_{2f1})} \tag{32}$$

and suppose that if $m > L$ or $g(\omega_{2f1}, \omega_{2f2}) < g_L$ the iterative process terminates. The flow process chart of the algorithm is shown in Fig. 3, where $\mathrm{sgn}(\cdot)$ is the symbolic function, that is,

$$\mathrm{sgn}(x) = \begin{cases} 1 & x \geq 0 \\ -1 & x < 0 \end{cases}$$

Let the eccentricity, inclination, right ascension of the ascending node, and initial mean anomaly of the deputy corresponding to ω_2^* be e_2^*, i_2^*, Ω_2^*, and M_{20}^*, respectively. Then the estimation value of

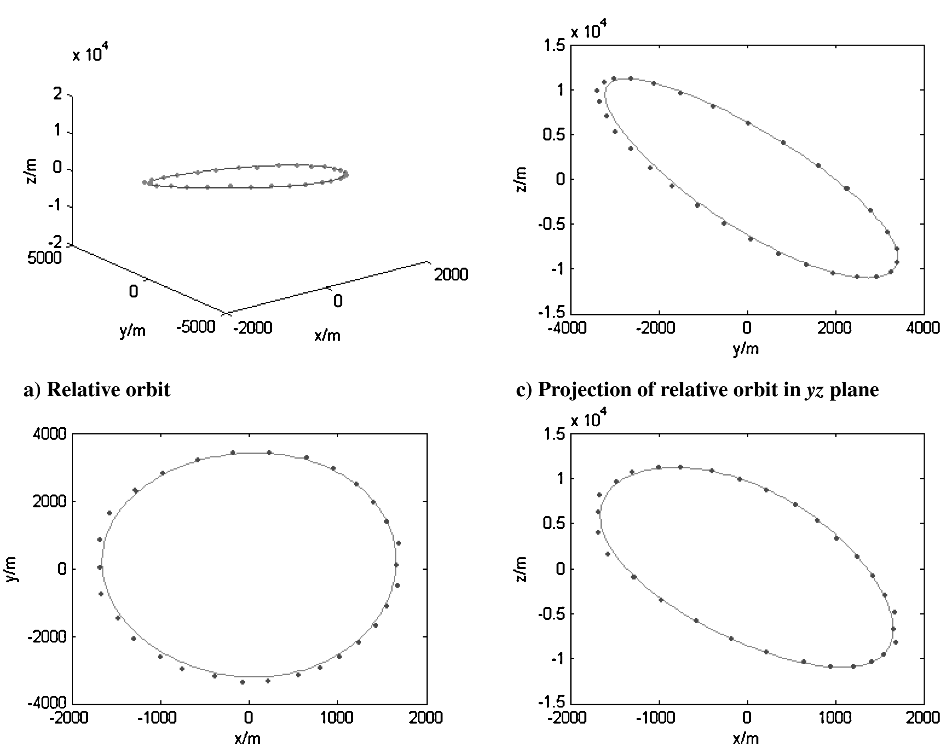

a) Relative orbit

c) Projection of relative orbit in *yz* plane

b) Projection of relative orbit in *xy* plane

d) Projection of relative orbit in *xz* plane

Fig. 4 Relative orbits: - - - -, measured and ——, calculated.

Table 1 Measurement relative position coordinates of 30 points on actual relative orbit

Number	x, km	y, km	z, km	Number	x, km	y, km	z, km	Number	x, km	y, km	z, km
1	−1.2942	2.2801	−1.0632	11	1.6553	0.7227	−8.2576	21	−0.0849	−3.3037	9.8032
2	−0.9587	2.8499	−3.5588	12	1.6933	0.1271	−6.7008	22	−0.4001	−3.2259	10.6897
3	−0.5929	3.2016	−5.8336	13	1.6344	−0.4930	−4.8995	23	−0.7024	−2.9679	11.1376
4	−0.2095	3.4104	−7.8215	14	1.5536	−1.1474	−2.9194	24	−1.0148	−2.6137	11.1095
5	0.2271	3.3943	−9.3456	15	1.4509	−1.6818	−0.8507	25	−1.3108	−2.1012	10.6184
6	0.6256	3.2869	−10.3920	16	1.2567	−2.1662	1.2542	26	−1.4514	−1.4654	9.6337
7	0.9291	2.9348	−10.8900	17	1.0466	−2.5778	3.3000	27	−1.6661	−0.7696	8.1054
8	1.1902	2.5104	−10.8956	18	0.8142	−2.9668	5.2909	28	−1.6892	0.0129	6.2274
9	1.4309	1.9657	−10.4439	19	0.5614	−3.1852	7.0888	29	−1.6700	0.8307	4.0050
10	1.5654	1.3727	−9.5389	20	0.2200	−3.3027	8.5877	30	−1.5311	1.6040	1.5276

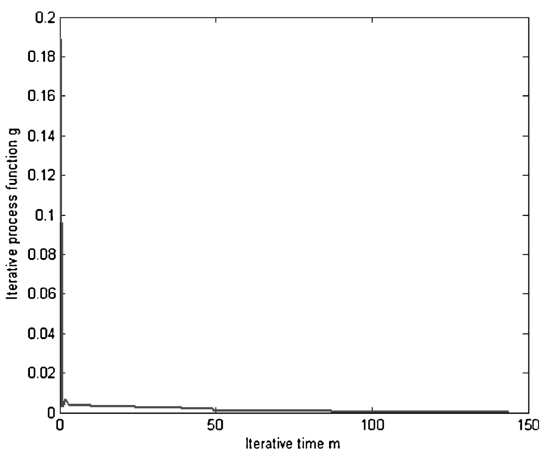

Fig. 5 Iterative function values in iterative process.

the orbit element difference vector $[\Delta a\ \Delta e\ \Delta i\ \Delta\Omega\ \Delta\omega\ \Delta M_0]^T$ can be represented as

$$\begin{bmatrix} \Delta a \\ \Delta e^* \\ \Delta i^* \\ \Delta\Omega^* \\ \Delta\omega^* \\ \Delta M_0^* \end{bmatrix} = \begin{bmatrix} a \\ e_2^* \\ i_2^* \\ \Omega_2^* \\ \omega_2^* \\ M_{20}^* \end{bmatrix} - \begin{bmatrix} a \\ e_1 \\ i_1 \\ \Omega_1 \\ \omega_1 \\ M_{10} \end{bmatrix} = \begin{bmatrix} 0 \\ e_2^* - e_1 \\ i_2^* - i_1 \\ \Omega_2^* - \Omega_1 \\ \omega_2^* - \omega_1 \\ M_{20}^* - M_{10} \end{bmatrix} \tag{33}$$

Simulation Results

Let the orbit elements of the chief $[a\ e_1\ i_1\ \Omega_1\ \omega_1\ M_{10}]^T = [2R_E\ 0.1\ 60\ \text{deg}\ 10\ \text{deg}\ 6\ \text{deg}\ 0\ \text{deg}]^T$, where R_E is the radius of the Earth. We select 30 different points of an actual relative orbit in the LVLH coordinate frame, and the coordinates are listed in Table 1. Let $L = 200$, $d\omega_{2f} = 0.0005$ deg and $g_L = 1 \times 10^{-4}$. By the use of the approach presented in earlier sections, we can obtain that $[a\ e_2\ i_2\ \Omega_2\ \omega_2\ M_{20}]^T = [2R_E\ 0.1001\ 60.05\,\text{deg}\ 10\,\text{deg}\ 5.9527\,\text{deg}\ 0.0485\,\text{deg}]^T$ and $[\Delta a\ \Delta e\ \Delta i\ \Delta\Omega\ \Delta\omega\ \Delta M_0]^T = [0, 0.0001\ -0.05\,\text{deg}\ 0\,\text{deg}\ -0.0487\,\text{deg}\ 0.0485\,\text{deg}]^T$. The measurement and calculated relative orbits are shown in Fig. 4. The values of the iterative process function g in the iterative process are shown in Fig. 5.

The differences between the orbit elements of the deputy and that of the chief utilized to generate the relative position coordinates are given as $[\Delta a\ \Delta e\ \Delta i\ \Delta\Omega\ \Delta\omega\ \Delta M_0]^T = [0, 0.0001\ -0.05\,\text{deg}\ 0\,\text{deg}\ -0.05\,\text{deg}\ 0.05\,\text{deg}]^T$, and the measurement relative position coordinates are the generated relative position coordinates with the measurement noise $\boldsymbol{n}_k$. Note that the measurement noise $\boldsymbol{n}_k \in R^3$ has the following statistical properties: $E[\boldsymbol{n}_k] = \boldsymbol{0}_{3\times 1}$ and $E[\boldsymbol{n}_k \boldsymbol{n}_l^T] = 100\boldsymbol{I}_3\delta_{kl}$, where δ_{kl} is the Kronecker delta function, which is equal to unity for $k = l$ and zero elsewhere. From the simulation results, we can see that there is no error between the estimation and actual values of the differences of eccentricity, inclination, and right ascension of the ascending node, and the calculated errors of the differences of initial mean anomaly and argument of perigee are 0.0013 and −0.0015 deg, respectively. Thus, the method presented in this paper is feasible.

Conclusions

In this Note, the relationship between the relative orbit and the classical orbit elements of the deputy is presented, and a least-squares estimation method for estimation values of Ω_2, i_2, e_2, and M_{20} is proposed on the assumption that the values of the deputy's argument of perigee and relative position coordinates of $N\,(N \geq 4)$ different points on the actual orbit are given and the chief's orbit elements are known. Moreover, a searching algorithm that gives searching value of the deputy's argument of perigee is proposed. Finally, the simulation results show that the method presented in this paper can be utilized to determine the classical orbit element differences between the chief and deputy. Because of the utilization of the relative position coordinates, this approach can be used to identify a satellite's orbit elements using the intersatellite baseline measurement device of another satellite.

References

[1] Tillerson, M., Inalhan, G., and How, J. P., "Co-Ordination and Control of Distributed Spacecraft Systems Using Convex Optimization Techniques," *International Journal of Robust Nonlinear Control*, Vol. 12, No. 2–3, 2002, pp. 207–242.

[2] Campbell, M. E., Zanon, D., and Kuldarni, J., "Cluster Planning and Control for Spacecraft Formations," American Astronautical Society, AAS Paper 04-254, Feb. 2004.

[3] Schaub, H., "Relative Orbit Geometry Through Classical Orbit Element Differences," *Journal of Guidance, Control, and Dynamics*, Vol. 27, No. 5, 2004, pp. 839–848.

[4] Schaub, H., Vadali, S. R., and Alfriend, K. T., "Spacecraft Formation Flying Control Using Mean Orbit Elements," *Journal of the Astronautical Sciences,* Vol. 48, No. 1, 2000, pp. 69–87.

[5] Schaub, H., and Alfriend, K. T., "Impulsive Feedback Control to Establish Specific Mean Orbit Elements of Spacecraft Formations," *Journal of Guidance, Control, and Dynamics*, Vol. 24, No. 4, 2001, pp. 739–745.

[6] Naasz, B. J., Karlgaard, C. D., and Hall, C. D., "Application of Several Control Techniques for the Ionospheric Observation Nanosatellite Formation," American Astronautical Society, AAS Paper 02-188, Jan. 2002.

[7] Alfriend, K. T., Schaub, H., and Gim, D.-W., "Gravitational Perturbations, Nonlinearity and Circular Orbit Assumption Effect on Formation Flying Control Strategies," American Astronautical Society, AAS Paper 00-012, Feb. 2000.

[8] Gim, D.-W., and Alfriend, K. T., "State Transition Matrix of Relative Motion for the Perturbed Noncircular Reference Orbit," *Journal of Guidance, Control, and Dynamics*, Vol. 26, No. 6, 2003, pp. 956–971.

[9] Schaub, H., and Alfriend, K. T., "Hybrid Cartesian and Orbit Element Feedback Law for Formation Flying Spacecraft," *Journal of Guidance, Control, and Dynamics*, Vol. 25, No. 2, 2002, pp. 387–393.

C. McLaughlin
Associate Editor